Technical Paper

Journal Bearing Vibration and SSV Hash

Presented at the Thirty-Seventh Turbomachinery Symposium, 2008

Kingsbury, Inc.®

Over 100 Years of Bearing Innovation

ABSTRACT

Peculiar, low-frequency, radial vibrations have been observed in various turbomachinery using tilt-pad journal bearings. Unlike discrete subsynchronous spikes that often indicate a serious problem, the vibrations are indiscrete and of low frequency and amplitude. The low level shaft indications have raised concern in witness tests of critical machinery, even in cases that comply with American Petroleum Institute (API) limits, owing to uncertainty regarding the cause and nature of the vibrations.

This paper presents shaft and pad vibration data from various tilt-pad journal bearing tests that were undertaken to investigate and better understand these subsynchronous indications. The vibration characteristics are defined and compared under the influence of speed, load, oil flow, and bearing orientation. Results are presented for conventional and direct lube tilt-pad bearing designs, along with discussions of parameters and methods that were successful in reducing and eliminating these low level vibrations.

The test results indicate that the low-frequency shaft indications are caused by pad vibration. Hypotheses and analyses are presented and discussed in relation to the test observations.

INTRODUCTION

Many early technical papers report on the inherent stability of tilt-pad journal bearings in overcoming oil whirl and oil whip limitations of fixed geometry bearings. There are, however, other vibration phenomena associated with tilt-pad bearings that are topics of past and present research. In the late 70s, extensive babbitt fatigue cracking of upper, unloaded pads was a major problem in large, conventional tilt-pad journal bearings. These were *flooded* designs, which incorporate end seals to restrict oil outlet and flood the bearing cavity. A well-referenced study by Adams and Payandeh (1983) attributes the damage to self-excited, subsynchronous pad vibration.

Trends for larger and higher speed turbomachinery impose greater demands on bearings and rotor dynamics. Direct lube bearings have evolved to reduce the higher power losses, oil flow requirements, and pad temperatures associated with higher surface speeds. Direct lubrication is not a new concept as designs have been used in special applications with a long history of reliability. Use of direct lube journal bearings became more prevalent as machine size and speed increased, eventually spawning several papers in the early 90s investigating their steady-state performance. These include research by Booser (1990), Tanaka (1991), Harongozo, et al. (1991), Brockwell, et al. (1992), and Fillon, et al. (1993).

The references document pad temperature reductions derived from the efficient evacuation of hot oil from the bearing cavity. Direct lube bearings are therefore typically designed for *evacuated* operation, accomplished by opening up end seal and oil outlet restrictions. A direct application of oil to the journal surface prevents oil from bypassing the films, which can occur in conventional bearings when outlet restrictions are removed. Use of nozzles to spray oil on the journal surface between pads is one method of direct lubrication. An additional pad temperature advantage is gained by direct lubrication features.

Literature on vibration characteristics of direct lube journal bearings is not as prevalent. DeCamillo and Clayton (1997) present rotordynamic data for large, 18 inch (457 mm) generator bearings. The tests showed comparable vibration response for conventional and direct lube designs. Edney, et al. (1996), provide similar information for a small, high-speed, multistage steam turbine with 4 inch (102 mm) diameter journal bearings. Peculiar, low-frequency, radial vibrations were observed during these steam turbine tests, but levels were low and acceptable. However, similar vibrations in a high-speed compressor during acceptance tests in 1999 did encroach upon acceptable API limits, and significant time and resources were expended to address this issue (DeCamillo, 2006).

Personal experience and discussions among original equipment manufacturers (OEMs) and users over the past few years indicate that these low-frequency vibrations have been encountered in turbines, compressors, and gearboxes, using conventional and direct lube tilt-pad bearing designs. The signature has also been documented in separate research investigating stability (Cloud, 2007). Accurate stability prediction is a major topic of concern in the industry. Kocur, et al. (2007), highlight a large spread in predicted bearing stiffness and damping coefficients among computer codes, and associated ramifications regarding stability assessment of critical turbomachinery. At the same time, there are not many codes available that address direct lube performance and dynamic coefficients (He, 2003; He, et al., 2005).

Researchers are presently attempting to sort through some difficult questions. What is the source of the low-frequency vibrations? Are they attributable to direct lube bearings, pad flutter, starvation, high speeds, or low loads? Do they affect machine stability, safety, or reliability?

This paper presents a chronology of tests, investigations, and theoretical analyses aimed at providing answers to some of these questions. It is desired that the information be of value to researchers, OEMs, users, and other personnel involved with hydrodynamic bearings and vibration in turbomachinery.

SSV HASH, DEFINITION

Figure 1 is an example radial vibration spectrum from a high-speed compressor test using direct lube tilt-pad journal bearings. The main subject of this paper is the low-frequency shaft vibrations indicated in the figure. Unlike discrete subsynchronous spikes that often indicate a serious problem, the vibrations are indiscrete and of low-frequency and amplitude. The plot is paused to capture the random, broadband frequencies. In order to distinguish the subsynchronous vibration (SSV) characteristics under consideration, the term *SSV hash* is defined for use in this paper:

- *SSV Hash: A vibration signature characterized by low-frequency, low amplitude, broadband subsynchronous vibrations that fluctuate randomly.*

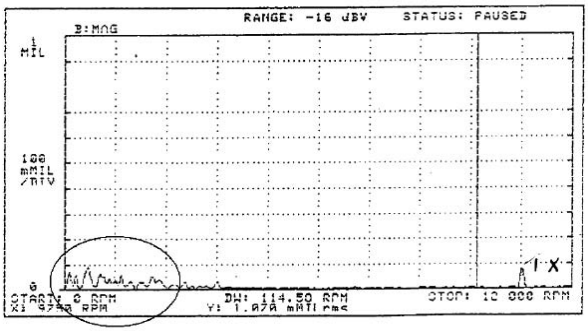

Figure 1. Example Radial, Low-Frequency, Broadband, Vibration.

Experience with turbomachinery bearing sizes 3.88 to 8.00 inches (100 to 200 mm) in diameter has observed SSV hash frequencies typically ranging up to 30 Hz with amplitudes on the order of 0.1 to 0.2 mils (.0025 to .0050 mm) peak-to-peak.

INITIAL INVESTIGATIONS

Delayed acceptance of a high-speed compressor due to SSV hash in 1999 prompted a research project performed on a high-speed test rig described in detail in a separate reference (Wilkes, et al., 2000). Pertinent information is provided here for convenience. The rig has a test shaft driven by a variable speed gas turbine through a flexible coupling (Figure 2). The test shaft is approximately 5 feet (1.5 m) long and 5 inches (127 mm) in diameter, supported at either end by a pivoted shoe journal bearing. Two orthogonal proximity probes are mounted inboard of each journal bearing, ± 45 degrees off top-dead-center, to record radial shaft vibration. A spectrum analyzer was used to acquire fast Fourier transform (FFT) vibration

signatures, presented in paused plots in Figures 3 through 5. The y-axis represents peak-to-peak amplitude in mils.

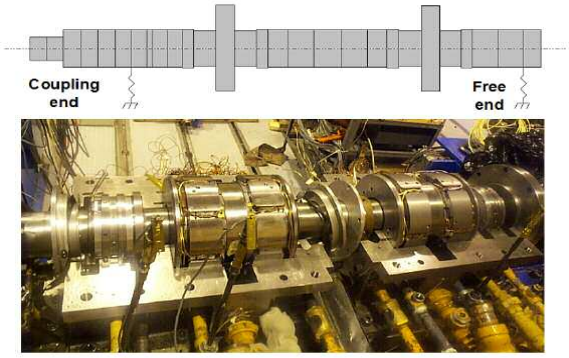

Figure 2. High-Speed Test Rig Journal Bearings and Shaft Schematic.

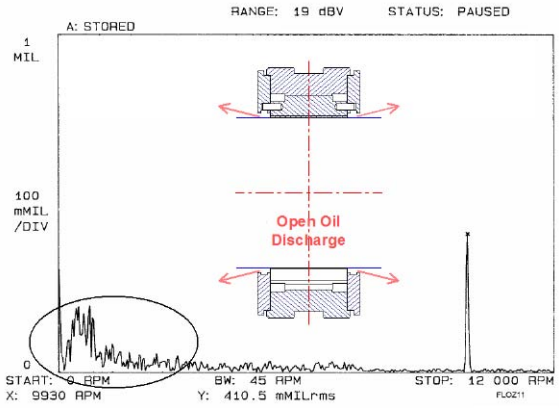

Figure 3. Evacuated Discharge Configuration, 3.0 gpm (11.4 l/min).

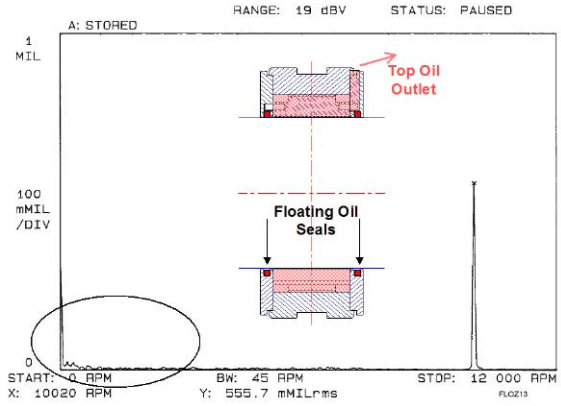

Figure 4. Flooded Discharge Configuration, 6.0 gpm (22.8 l/min).

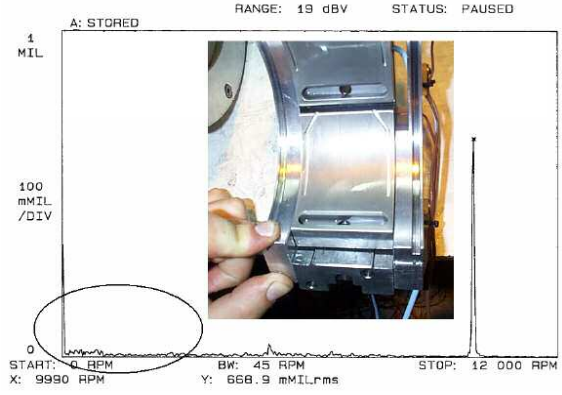

Figure 5. Evacuated Discharge Configuration, 3.0 gpm (11.4 l/min), SSV Grooves.

Fortunately, it was possible to duplicate the low-frequency vibration signature in the test rig, which allowed a parametric study of many journal bearing designs and configurations over the course of this initial investigation. The data presented in Figures 3 through 5 are for direct lube, five-pad, leading-edge-groove journal bearing tests at a shaft speed of 10,000 rpm and a low, 20 psi (0.14 MPa) projected load. The bearings have a nominal diameter of 5 inches (127 mm) and an axial length of 2.25 inches (57 mm). The pads are steel backed with a babbitt surface and have a 60 degree angle and a 60 percent offset pivot. The assembled bearing diametric clearance is 0.009 inch (0.23 mm) and the nominal preload is 0.15. Tests were run with ISO VG 32 turbine oil supplied at 120°F (49°C).

The SSV hash indicated in Figure 3 was recorded for an oil flow of 3.0 gpm (11.4 l/min) for the direct lube bearing in its as-designed, evacuated oil discharge configuration. Tests found that increasing the oil flow tended to reduce the amplitudes but did not entirely eliminate the SSV hash signature. Elimination required the installation of floating oil seals as well as an increase in oil flow to 6.0 gpm (22.8 l/min), the results of which are shown in Figure 4. This solution unfortunately required higher oil flow and operated with higher power loss and pad temperatures than the original design.

Methods were therefore pursued to address these performance issues, and results began to suggest that the low frequencies may be due to air entering the oil film. Based on this hypothesis, a design was conceived that might eliminate SSV hash while maintaining some direct lube benefits. The pads were modified with narrow circumferential *SSV grooves*, cut in the babbitt near the edges of the pads (Figure 5), to capture and redirect side leakage toward the leading edge of the next pad (Wilkes and DeCamillo, 2002). In this way, additional oil is made available to the oil films without increasing the bulk oil flow to the bearing.

The SSV groove pads were installed and tested in the original evacuated condition (oil seals removed) with results shown in Figure 5 for 3.0 gpm (11.4 l/min), and tested as low as 2.0 gpm (7.6 l/min) with negligible SSV hash indications. Of several methods pursued during the course of this initial investigation, the grooves were the only solution successful in eliminating SSV hash in an evacuated configuration. The low oil flow and power loss of the original design were maintained, with a slight penalty in pad temperature due to the introduction of warm, side leakage oil back into the oil film.

Another observation of this initial investigation was the tendency for an increase in synchronous amplitudes when SSV hash was eliminated, noticeable by comparing both the flooded solution (Figure 4) and the evacuated groove solution (Figure 5) with the original open discharge configuration data of Figure 3.

SUBSEQUENT TESTS

Although solutions were obtained in initial investigations, operating conditions were limited in load and speed. A subsequent series of tests was initiated in 2005 to further investigate the low-frequency vibrations. The same test rig was modified to incorporate a radial load system in the bearing housing at the free end of the shaft, shown schematically in Figure 6. The system incorporates a hydraulic cylinder that loads through a dowel to a single journal bearing loader shoe on top of the shaft. This pushes down on the shaft and loads the test bearing. The applied load is measured by a load cell below the hydraulic cylinder. A new data acquisition system was used to acquire the data, and additional proximity probes were installed to monitor the vibration of an upper and a lower journal bearing pad. The pad proximity probes were mounted in the bearing casing and targeted the trailing edge of the back of the pads at the locations depicted schematically in Figure 7.

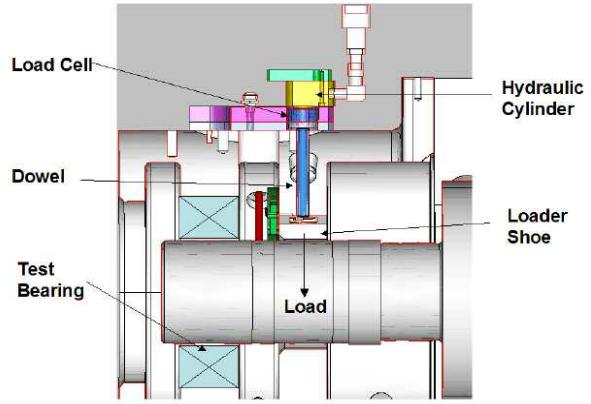

Figure 6. Test Rig Radial Load System Schematic, Free End of Shaft.

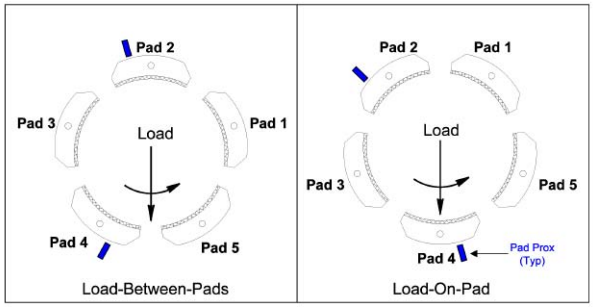

Figure 7. Bearing Orientation and Pad Numbering.

The test bearings consist of a conventional center pivot bearing with labyrinth end seals (Figure 8) and evacuated direct lube center and offset pivot bearings. Three direct lube methods were tested: spray nozzles (Figure 9), leading-edge-grooves (Figure 10), and between-pad-grooves (Figure 11). Each bearing was tested for load-on-pad and load-between-pad orientation over a range of loads, oil flows, and speeds.

Figure 8. Conventional Bearing with Labyrinth End Seals.

Figure 9. Direct Lube Spray Nozzles, Evacuated Configuration.

Figure 10. Direct Lube Leading-Edge-Groove, Evacuated Configuration.

Figure 11. Direct Lube Between-Pad-Groove, Evacuated Configuration.

Bearing geometry, test oil viscosity, and inlet temperature are the same as in earlier investigations except that the assembled diametric clearance is 0.0072 inch (0.18 mm) and the nominal preload is 0.25. Loads indicated in the following sections and figures refer to the applied radial load. For data labeled no-load, the journal bearings are supporting the weight of the shaft, which gives a 20 psi (0.14 MPa) projected unit bearing load. Each test bearing is installed around the free end of the shaft without disturbing the coupling or the coupling end journal bearing. The same coupling end journal bearing is used in all tests. Vibration data were recorded while varying speed to 14,000 rpm, load to 400 psi (2.8 MPa), and oil flow to 30 gpm (114 l/min), holding two of the parameters constant while the other was varied.

The speed ramp data are used in this paper, presented in color-coded FFT waterfall diagrams with a vertical scale denoting peak-to-peak amplitude in mils. With Figure 12 as an example, each waterfall diagram contains data for three separate run-up/run-down speed ramps from 5000 to 14,000 to 5000 rpm (83 to 233 to 83 Hz), one for each of three oil flows. The back plane of the diagram contains a projection of all data. Vibrations below 1 Hz are cut off to delete spurious 0 Hz indications from obscuring the low frequencies under investigation and the data are uncompensated, the main focus being the low-frequency vibrations. As a guide, SSV hash amplitudes above 0.1 mils (0.0025 mm) peak-to-peak are levels that have caused concern in acceptance tests.

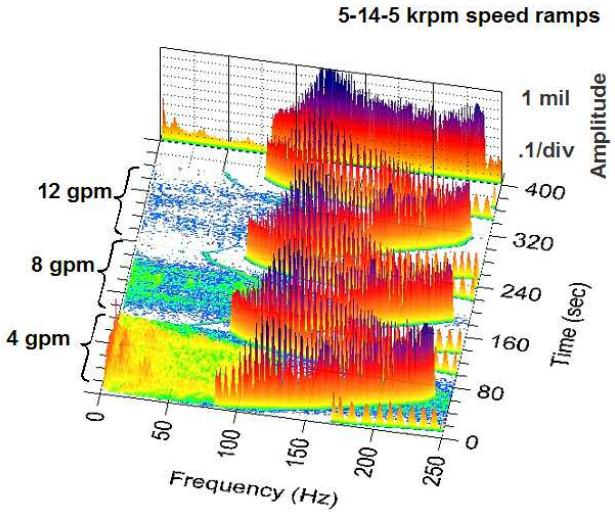

Figure 12. Conventional Center Pivot, LBP, No-Load.

Shaft SSV Hash Trends

The volume of data for the different bearing designs allowed for an assessment of trends in shaft SSV hash. This section describes those that were fairly common for all test bearings. Conventional bearing speed ramp data in Figures 12 through 15 are used for reference.

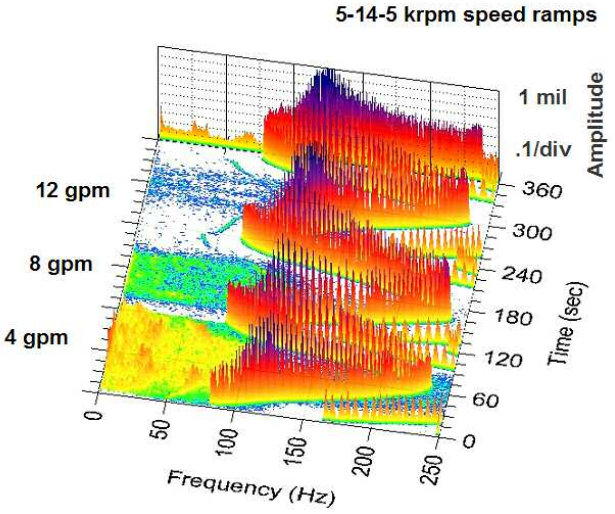

Figure 13. Conventional Center Pivot, LOP, No-Load.

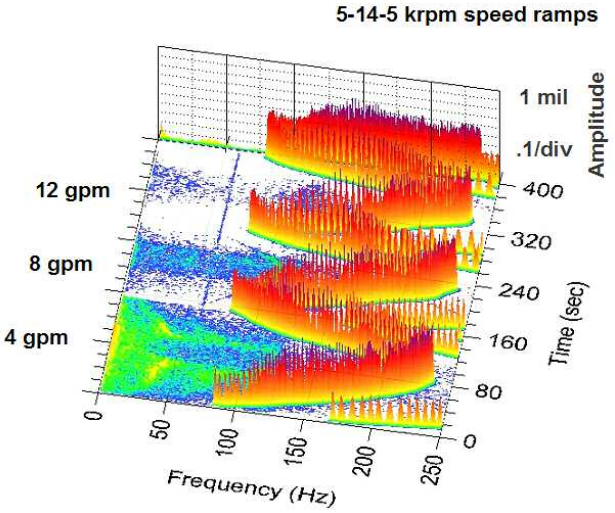

Figure 14. Conventional Center Pivot, LBP, 400 psi (2.8 MPa).

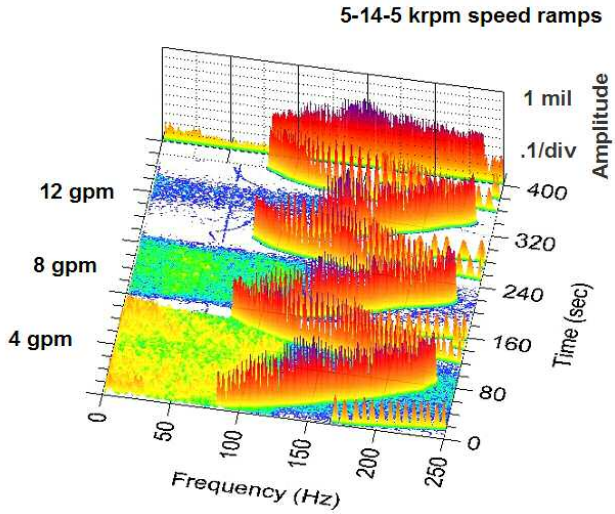

Figure 15. Conventional Center Pivot, LOP, 400 psi (2.8 MPa).

Comparing data among the figures, it can be noticed that most SSV hash indications occur at low flow and low load. The word "indications" is carefully used in this generalization. Although there were more indications at low flow and low load for most bearing designs, SSV hash *amplitudes* were sometimes higher at other operating conditions, as evidenced in results later in this paper.

Other common trends derived from the study are that SSV hash levels for no-load data were similar for load-between-pad (LBP) and load-on-pad (LOP) orientations (e.g., Figures 12 and 13). A curious result was that while SSV hash decreased with applied load for load-between-pad orientation (e.g., Figure 12 versus 14) there was only a small change with load for load-on-pad orientation (e.g., Figure 13 versus 15). Consequently, load-on-pad orientation had higher SSV hash levels than load-between-pad orientation at higher loads for all test bearings.

It is worth noting that initial investigations and field reports were for high-speed applications with relatively light rotors, and so SSV hash was formerly associated with high-speed and low-load. The test data in these subsequent series of tests indicate that this is not exactly true. Although indications were more pronounced at low loads, tests indicate there can be undesirable levels of SSV hash in the case of load-on-pad orientation at higher loads, for example Figure 15 at 400 psi (2.8 MPa). There were also many indications at lower speeds in the test data, again using Figure 15 as an example.

Conventional Versus Direct Lubrication

Figure 16 displays no-load data for the conventional center pivot test bearing with load-on-pad orientation, the same used in Figure 13, but zoomed in on the lower frequencies and amplitudes under investigation. Figure 17 contains comparable, center pivot, between-pad-groove direct lube data. A condition mentioned earlier is noticeable in the direct lube data, i.e., there are more SSV hash indications at low flow but with higher amplitudes at an intermediate condition, 8 gpm (30 l/min) and 11,000 rpm in this particular test. The figure also supports observations from field experience and initial investigations where SSV hash decreases, but is not necessarily eliminated at higher flows.

Comparisons between conventional and direct lube results (Figures 16 and 17) are fairly straightforward. Direct lube data have noticeable SSV hash indications at 8 gpm (30 l/min) whereas conventional bearing levels are negligible. Conversely, very high subsynchronous vibrations are noticeable in conventional bearing data at 4 gpm (15 l/min) where the direct lube design has significantly lower SSV hash indications.

These data indicate that flooding and oil flow are not the only key parameters influencing SSV hash. Conventional bearing tests with labyrinth seals (Figure 16), and initial tests with oil seal rings

(Figure 4), both required some increase in oil flow to eliminate the signature, whereas higher oil flow is not as effective in evacuated designs (e.g., Figure 17). This suggests cavity pressure may be another influential parameter that, unfortunately, was not measured. Calculated pressure drops across oil discharge restrictions indicate that cavity pressures between 0.5 and 2.0 psig (0.04 and 0.14 bar) were present when SSV hash was noticeably reduced. Also fitting this scenario are the lower SSV hash indications in direct lube designs compared to the conventional bearing data at low flow (Figure 17 versus 16), which may be attributable to the more direct application of oil to the oil films.

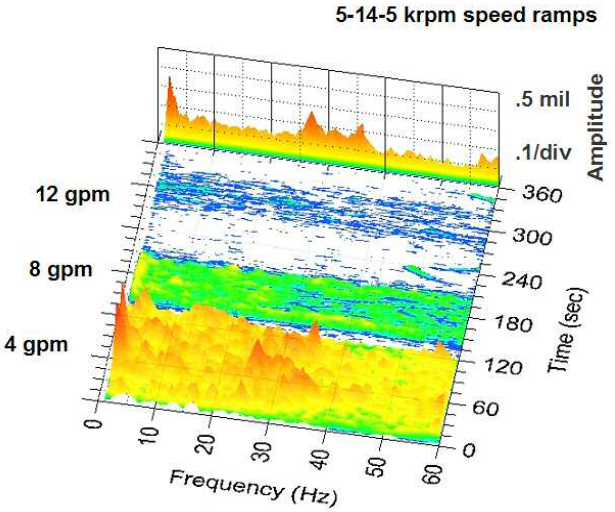

Figure 16. Conventional Center Pivot, LOP, No-Load.

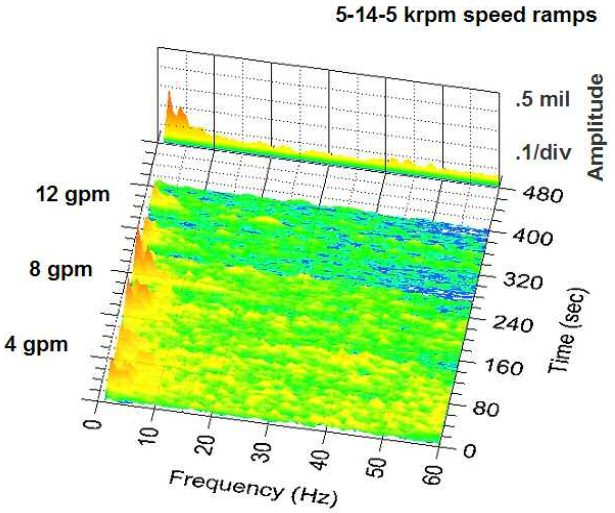

Figure 17. Direct Lube Between-Pad-Groove, Center Pivot, LOP, No-Load.

Center Versus Offset Pivot

Center versus offset pivot tests were conducted for several direct lube bearing configurations. Comparisons have been difficult to quantify. For example, spray nozzle offset pivot data (Figure 18) have high amplitudes and a broad band of SSV hash midway through the 4 gpm (15 l/min) data speed ramps at approximately 12,000 rpm, indicated in the figure. At the same conditions, spray nozzle center pivot data (Figure 19) have less broadband indications, and amplitudes are actually highest at approximately 6000 rpm. In 8 and 12 gpm data (30 and 45 l/min), the offset pivot has slightly less SSV hash. Similar comparisons for between-pad-groove tests (Figure 17 versus 20) show lower SSV hash levels in the offset pivot data at 4 gpm (15 l/min), and only subtle differences at the higher flows.

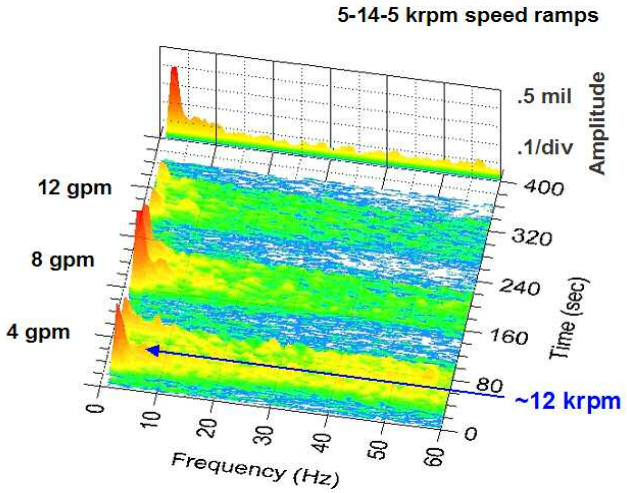

Figure 18. Direct Lube Spray, Offset Pivot, LOP, No-Load.

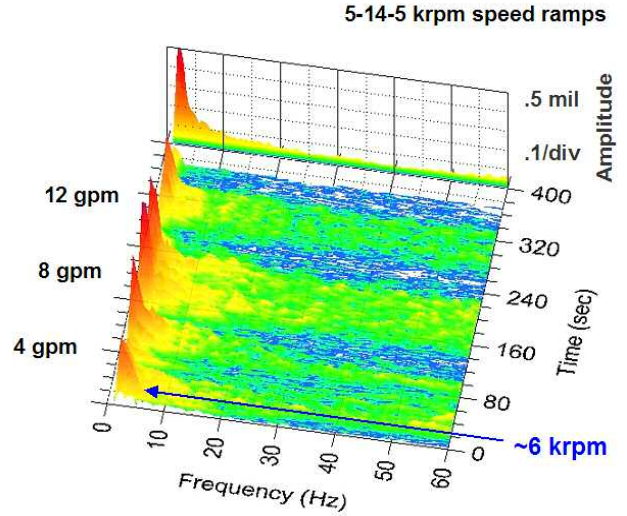

Figure 19. Direct Lube Spray, Center Pivot, LOP, No-Load.

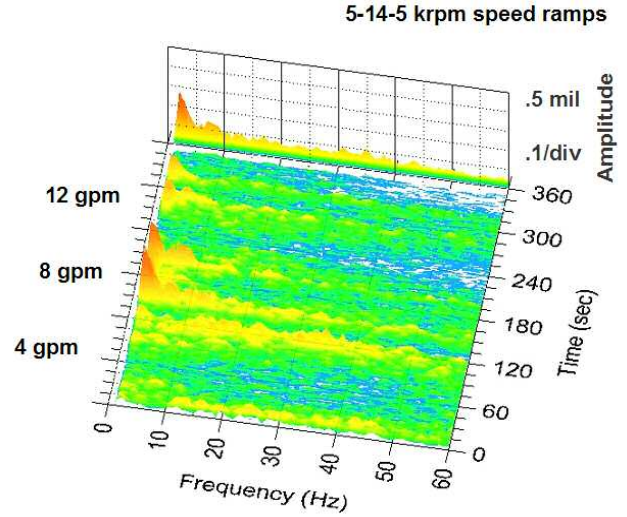

Figure 20. Direct Lube Between-Pad-Groove, Offset Pivot, LOP, No-Load.

The results were unexpected in that offset pivot designs require more oil flow to the films, and it was suspected that this would be clearly reflected in SSV hash levels. The data indicate there are factors other than bulk oil flow that need to be taken into account regarding SSV hash and pivot offset.

Variations Among Direct Lube Designs

Three offset pivot, direct lube bearings were tested to compare shaft SSV hash characteristics among different methods of direct lubrication. All three have an evacuated discharge configuration. The methods include spray nozzles, leading-edge-grooves, and between-pad-grooves. Photographs of the direct lube features are provided in Figures 9 through 11, and corresponding vibration data are contained in Figures 19 through 21.

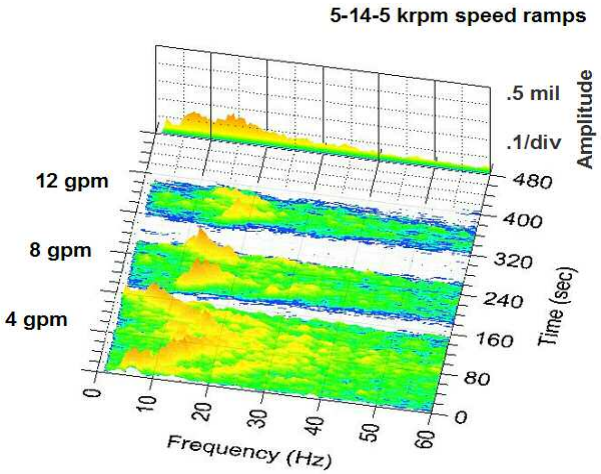

Figure 21. Direct Lube Leading-Edge-Groove, Offset Pivot, LOP, No-Load.

In general, all three direct lube methods display noticeable SSV hash indications. Variations in amplitudes and frequencies make it difficult to generalize the results. The spray nozzles produced the highest levels of SSV hash. The leading-edge-groove operated with lower SSV hash amplitudes but at higher frequencies, and between-pad-groove SSV hash levels were lower for all conditionsin comparison with spray nozzle data. Results comparing between-pad-groove and leading-edge-groove data vary with operating conditions. SSV hash levels at 4 gpm (15 l/min) are negligible and lower than the leading-edge-groove. At higher flows, between-pad-groove SSV hash amplitudes are higher but occur at a lower frequency.

Distinct differences in shaft SSV hash signatures are obvious among the designs. Some speed dependence is noticeable in spray nozzle data (Figure 18), and more so in leading-edge-groove data (Figure 21), which appears to be suppressed at higher speeds. Between-pad-groove characteristics (Figure 20) do not show variations with speed, and seem sensitive to a particular speed band depending on flow. There are also many conditions throughout Figures 18 through 21 where the evacuated direct lube bearings operate with negligible SSV hash indications.

While the reasons for the variations are still under investigation, the fact that there are differences provides valuable information. Since the pad geometry is the same for the different bearings, the direct lube feature itself is influencing the shaft SSV hash and, because these are evacuated designs, the influence is most likely occurring at the entrance or leading edge of the oil film.

Pad/Shaft Correlation Investigation

A review of 2005 vibration data from the upper and lower pad proximity probes (depicted in Figure 7), noted more subsynchronous indications in the upper pad, with the highest amplitudes occurring at high-load and low-flow conditions in many cases. This is reasonable considering that the upper pad clearance increases as the shaft is pushed down under load, away from the upper pad. The upper pad oil film consequently generates lower hydrodynamic forces and requires more oil flow to fill the gap. Unfortunately, an unexpected result of the investigation was that there were only a few random correlations between upper pad and shaft SSV hash for the broad range of operating conditions and bearing configurations tested.

This lack of correlation prompted another series of tests in 2006 with all pads monitored by proximity probes, installed and positioned as described earlier, and made possible by the acquisition of new high-speed vibration equipment. Figure A-1 (refer to APPENDIX A) organizes shaft and pad vibration data for a leading-edge-groove bearing test at 200 psi (1.38 MPa), for a load-on-pad configuration as an example. The waterfall diagrams are arranged so that data for the orthogonal shaft probes and all five pads can be viewed in relation to one another. The same scales are used for all waterfall diagrams in the figure. It is important to note that the shaft was removed and refurbished between 2005 and 2006 tests and a different coupling end journal bearing installed, so data are not comparable to information from earlier tests.

Referring to Figure A-1, it can be noticed that the subsynchronous vibrations in unloaded pad 2 at 4 gpm (15 l/min) do not correlate with either of the orthogonal shaft probes (labeled +45 degrees and −45 degrees in the figure). A unique observation is that the side pads 3 and 5, which were not monitored in previous tests, have the strongest subsynchronous vibrations and show excellent correlation with the shaft SSV hash indications.

Pad/Shaft Correlation General Trends

The observations from Figure A-1 relate to a specific bearing and set of operating conditions. Comparisons of data for all five pads, over a broad range of operating conditions for the different bearing designs allowed for a more precise assessment of pad/shaft interaction. The following observations and trends were determined to be fairly common for all test bearings.

All shaft SSV hash indications observed in these tests were confirmed to correlate with vibrations from at least one of the five pads. The converse is not true. There were many instances where subsynchronous vibrations from individual pads did not appear in any shaft data. An important observation is that the shaft SSV hash indications most often correlated with one or more of the side pads, depending on bearing type and orientation. The orientation and pad number schematic in Figure 7 is helpful in explaining the following observations and trends.

In the case of load-between-pad orientation under some light downward loading, side pad 1, side pad 3, or both tended to correlate with the shaft SSV hash indications. Upper pad 2 had more and higher subsynchronous vibration than the side pads in many cases, but rarely correlated with the shaft indications. Noted earlier, shaft SSV hash decreased with applied load in the case of load-between-pad orientation, which is reasonable considering the high horizontal stiffness of this orientation with the shaft supported between the two bottom pads. At the same time, pads 1, 2, and 3 become less strongly coupled to the shaft and may still experience subsynchronous vibrations, but with hydrodynamic forces too weak to affect the shaft.

For a load-on-pad orientation under some light downward loading, the side pads (1, 2, 3, and 5), individually or in combinations, tended to correlate with the shaft SSV hash indications. The correlation varied with bearing type and operating conditions, and is also likely influenced by any slight skew in applied load vector and differences in manufacturing heights of the individual pads for this particular orientation. Noted earlier, shaft SSV hash did not decrease as much with applied load for load-on-pad orientation, which is reasonable considering the weak horizontal stiffness for this orientation. Pad 3 and pad 5 tended to correlate more with the shaft SSV hash indications as load was applied. At the same time, pads 1 and 2 become less strongly coupled to the shaft and may still experience subsynchronous indications, but with hydrodynamic forces too weak to affect the shaft.

SSV Grooves, Recent Tests

The SSV groove modification (Figure 5), developed during initial investigations in 1999, has since been successfully applied in

many compressor, turbine, and gearbox applications. At the time, development was based on hypotheses and shaft vibration data. Upgrades in the test rig capability and in high-speed data acquisition equipment has more recently allowed an investigation of the groove's influence on pad vibration.

SSV grooves were machined in the leading-edge-groove pads used for results presented in Figure A-1 and were tested over the full range of operating conditions for load-on-pad and load-between pad orientation. Test results for the same conditions and orientation as Figure A-1 are presented in Figure A-2 (refer to APPENDIX A) as an example comparison. The tests found that subsynchronous levels in all pads were significantly reduced or eliminated over the full range of test operating conditions and configurations, and confirmed the effectiveness of the method in eliminating shaft SSV hash in evacuated, direct lube bearing designs.

THEORETICAL INVESTIGATIONS

To help shed some light on these SSV hash measurements, the bearing geometry and operating conditions corresponding with the data in Figure A-1 were modeled using an algorithm developed by He (2003). This algorithm includes the effects of supply flowrate in its determination of a bearing's steady-state (eccentricity, temperatures, power loss, etc.) and dynamic (stiffness and damping) performance based on the theories and experiments put forth by Heshmat (1991). Since the measurements presented in these SSV hash tests demonstrate the importance of supply flow on SSV, any theoretical investigation must account for supply flowrate effects.

Supply Flowrate Effects

The model applies to any bearing configuration where the supply flowrate is not sufficient to ensure a full film across all the pads' surfaces. In this case, the model will predict a partial starvation at the inlet region of some of the pads. Unlike the full film situation where a continuous lubricant film starts at the pad leading edge, in a partially starved situation, the continuous film is formed downstream at some point where the clearance is sufficiently reduced. This physical phenomenon was observed and studied by Heshmat (1991) on a two axial groove, sleeve bearing.

Figure 22 illustrates predicted starvation effects for pad number 3, corresponding with the test data pad numbers in Figure A-1. With a supply flowrate of 8 gpm to the bearing, the film is able to generate pressure across the pad's entire arc length. Reducing the bearing flow to 4 gpm lowers overall pressure distribution, but the pad still produces pressure across almost all of its arc length. The pad is clearly partially starved at 3 gpm where no film pressure is produced at the inlet film region. Decreasing the flow to 2 gpm expands the starved inlet region. At this flow level, pressure levels are very small and the pivot is nearly centered within the positive pressure region. Partial starvation has effectively reduced the pad's pivot offset, which may explain unexpected results in center versus offset pivot tests.

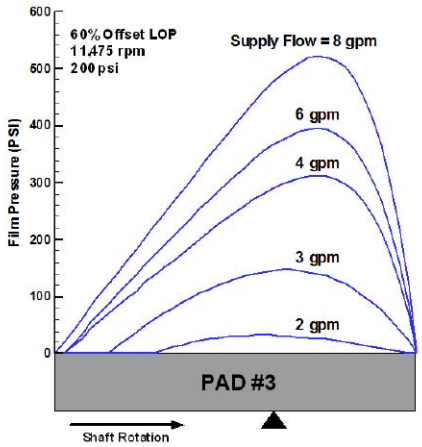

Figure 22. Partial Starvation Effects on Pad Film Pressure.

Pad Responsiveness

Since test results confirm that the individual pad motions are involved in this SSV hash phenomenon, the tilting-pad bearing's full coefficients predicted by the modeling algorithm are of primary interest. For a tilting-pad bearing with N_{pad} pads, the full coefficients consist of $5N_{pad}+4$ stiffness and $5N_{pad}+4$ damping coefficients. Described in detail by Shapiro and Colsher (1977) and Parsell, et al. (1983), these full coefficients relate pad and shaft motions to forces and moments on the shaft and pads. For rotordynamic purposes, the magnitude of each individual coefficient is overlooked, focusing instead on their combined or "reduced" coefficients (four stiffnesses and four dampings). Closer scrutiny and understanding of these full coefficients are required when pad dynamics become the focus.

Table 1 presents the stiffness full coefficients for a 60 percent offset, LOP, five-pad bearing with 12 gpm supply flowrate where:

ΔFx and ΔFy = Horizontal and vertical forces on the shaft
Δx and Δy = Horizontal and vertical shaft displacements
$\Delta M_1 \ldots \Delta M_5$ = Moments on pads 1 through 5
$\Delta\delta_1 \ldots \Delta\delta_5$ = Tilt angle changes on pads 1 through 5

Table 1. Stiffness Full Coefficients for the 60 Percent Offset LOP Bearing, 11,475 rpm, 200 psi.

	Δx (in)	Δy (in)	$\Delta\delta_1$ (rad)	$\Delta\delta_2$ (rad)	$\Delta\delta_3$ (rad)	$\Delta\delta_4$ (rad)	$\Delta\delta_5$ (rad)
ΔF_x (E6 lbf)	3.351	.885	.347	-.459	-1.413	.512	1.612
ΔF_y (E6 lbf)	-1.298	4.612	.616	.499	-.683	-3.261	-.302
ΔM_1 (E6 lbf-in)	-.029	.098	.265	0	0	0	0
ΔM_2 (E6 lbf-in)	-.097	.002	0	.245	0	0	0
ΔM_3 (E6 lbf-in)	-.104	-.258	0	0	.672	0	0
ΔM_4 (E6 lbf-in)	.512	-.469	0	0	0	1.614	0
ΔM_5 (E6 lbf-in)	.220	.150	0	0	0	0	.665

Each value in Table 1 represents a stiffness, either ΔFx or ΔM divided by Δx, Δy, or $\Delta\delta$ depending on the position in the table. Examining a few of these Table 1 coefficients will help explain the physical meaning behind them. Tilt angle changes of the fourth pad ($\Delta\delta_4$) produce the largest vertical force on the shaft (ΔF_y), since it has the highest value of $K_{y\delta}$ (−3.261e6 lbf/rad). This is due to the fourth pad being on the bottom, supporting the majority of the load. Conversely, tilt angle changes on the second pad, located in the upper half of the bearing, produce the smallest vertical force on the shaft ($K_{y\delta}$ = 0.499e6 lbf/rad). The fourth pad is also the most difficult to tilt with the highest tilting stiffness $K_{\delta\delta}$ value (1.614e6 lbf-in/rad), while the second pad is the easiest to tilt ($K_{\delta\delta}$ = 0.245e6 lbf-in/rad). Tilting motions of the other four pads do not *directly* cause any moments on the loaded pad. The pads can only effectively communicate to each other through the shaft.

Some of the full coefficients along with the pads' polar inertia (I_p) form the equation of motion for pad tilting. A simplified version of this equation, using a pad's tilting stiffness $K_{\delta\delta}$ and damping $C_{\delta\delta}$, is given by:

$$I_p\ddot{\delta} + C_{\delta\delta}\dot{\delta} + K_{\delta\delta}\delta = M_{ext} \quad \textbf{(1)}$$

where M_{ext} is an external moment being applied. This equation can be used to examine the frequency response characteristics of each pad's tilting motion. Each pad's frequency response function (FRF) $H(\omega)$ is given by:

$$H(\omega) \equiv \frac{\delta(\omega)}{M_{ext}(\omega)} = \left\{-\omega^2 I_p + j\omega C_{\delta\delta} + K_{\delta\delta}\right\}^{-1}\left[\frac{rad}{lbf-in}\right] \quad \textbf{(2)}$$

An FRF's magnitude indicates how responsive a pad is to external moments trying to excite it. Examining the predicted FRFs of each pad as a function of supply flowrate provides for a direct comparison with the pad waterfall diagrams of the test data.

Figure 23 presents the predicted H(ω) of pad 3 in Figure A-1 as an example, focusing on the low frequency region below 60 Hz. Regardless of flow, the frequency response remains relatively flat as a function of excitation frequency with no peaks present. This is because the pad's tilting motions remain overdamped for all the flowrates examined. An overdamped system (critical damping greater than 100 percent) has no damped natural frequency, resulting in no peaks in its response.

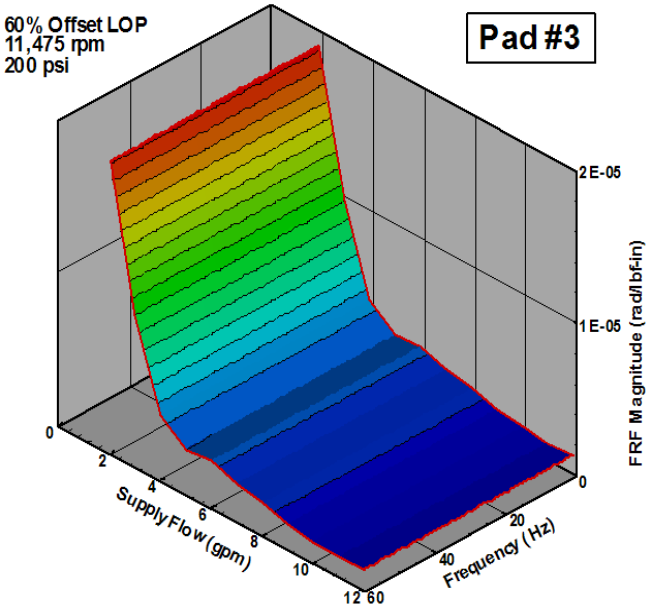

Figure 23. H(ω) with Decreasing Supply Flow.

It is unclear as to the exact cause of the 8 Hz peak in Figure A-1's waterfall diagram for pad 3. One explanation is that there may be a predominant excitation at this frequency. Heshmat (1991) observed a pulse excitation at similar low frequency levels in his starvation experiments on a sleeve bearing. Another possibility may be that the pad is actually underdamped, which the model has not been able to predict. In this case, a broadband excitation would result in a definitive peak at the pad's damped natural frequency. Nothing indicates that the peak is associated with an unstable, self-excited phenomenon, since the pad's tilting damping $C_{\delta\delta}$ remains greater than or equal to zero. All indications are that the observed vibrations are forced in nature.

Both the measurements in Figure A-1 and the predicted FRF in Figure 23 show that the third pad's overall responsiveness does dramatically increase as supply flow is reduced. According to the predictions in Figure 23, this pad responds very little to excitations until the bearing flow is reduced below approximately 4 gpm. This increased sensitivity correlates well with the predicted pressure profiles in Figure 22. Below 4 gpm, the predictions in Figure 22 show that the pad becomes partially starved at the leading edge with low overall film pressures. These lower film pressures allow the pad to respond to external moment excitations more easily.

According to the H(ω) equation, the low frequency responsiveness of an individual pad is largely dictated by its tilting stiffness, $K_{\delta\delta}$. Figure 24 presents the calculated tilting stiffness of all five pads as supply flow is varied. With the exception of the fourth pad, reducing supply flow causes a decrease in all the pads' tilting stiffnesses. Below 5 gpm, the fourth pad's stiffness begins to increase as it supports more of the entire bearing load. The strength of this tilting stiffness means the fourth pad does not easily respond to excitations, which correlates well with its relatively low vibrations in Figure A-1.

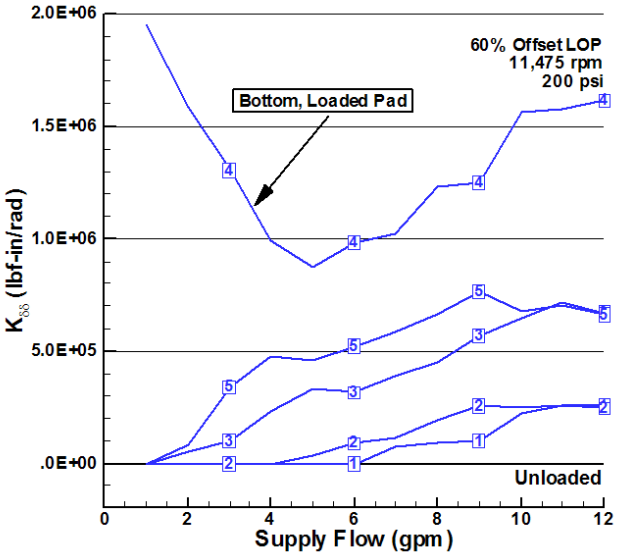

Figure 24. Tilting Stiffness of Individual Pads Versus Supply Flow.

When a pad becomes unloaded, it applies no pressure force on the shaft and its full coefficient stiffness and damping terms go to zero. The pad then moves like a rigid body and its tilting FRF is dictated by the polar inertia. The upper pads (1 and 2) become unloaded first as flow is reduced (Figure 24). This is because their larger film thicknesses require the most flow to maintain a full film along their entire surface. With smaller film thicknesses, the third and fifth pads remain loaded until below 2 gpm. These two pads' tilting stiffness values are low in magnitude at reduced flowrates, resulting in the increased responsiveness observed in Figure 23.

CONCLUSIONS

A series of tests and analyses were performed to investigate a peculiar, low-frequency, low amplitude, broadband subsynchronous vibration, termed *SSV hash*, that has been witnessed in different types of turbomachinery using tilting pad journal bearings.

Based on a study of test results for conventional and direct lube designs over a broad range of speeds, loads, and oil flows, the following shaft SSV hash trends were found to be fairly common for all test bearings:

- There were more SSV hash indications at low flow and low load, although amplitudes were sometimes higher at other operating conditions.
- SSV hash levels at light loads were similar for load-between-pad and load-on-pad bearing orientations.
- Shaft SSV hash decreased with applied load for load-between-pad orientation, but there was only a small change with load for load-on-pad orientation.
- Consequently, load-on-pad operation produced higher SSV hash levels than load-between-pad orientation at higher loads.

The following general trends for pad/shaft vibration correlation were found fairly common for all test bearings based on tests of bearing designs with vibration measurements of all five pads:

- All shaft SSV hash indications were confirmed to correlate with vibrations of at least one of the five pads.
- The converse is not true. There were subsynchronous vibrations in individual pads that did not appear in measured shaft vibration data.
- The side pads most often correlated with shaft SSV hash indications. The top upper pad for load-between-pad orientation had the highest subsychronous indications in many cases, but rarely correlated with any shaft data.

The following specific observations were noted in test data comparisons of bearing types and geometries:

- It is incorrect to associate SSV hash only with high-speed, low-load applications. Indications were noted over a broad range of operating conditions.
- Shaft SSV hash has been observed in conventional bearing designs at low oil flow. The data indicate that merely flooding the cavity is insufficient to suppress shaft SSV hash. At these conditions, direct lube designs operate with lower levels of shaft SSV hash, attributed to the more direct application of oil to the film.
- At intermediate test oil flows, shaft SSV hash is more pronounced in evacuated, direct lube bearings and can be reduced, but not necessarily eliminated, by increasing oil flow. Amplitudes appear sensitive to certain operating conditions, around which are conditions where the evacuated direct lube bearings operated with negligible SSV hash indications.
- There were mixed results in SSV hash comparisons of center versus offset pivot direct lube test data. The offset pivot pads in most cases operated with the same to slightly less SSV hash indications than the center pivot pads.
- Comparisons among three direct lube methods noted distinct differences in shaft SSV hash signatures, the results suggesting that the differences originate at the entrance or leading edge of the oil film.

Overall, the various tests and comparisons indicate there are factors other than flooding and bulk oil flow that contribute to SSV hash behavior.

There were two solutions determined from test data that eliminated the SSV hash signature:

- The first required flooding the bearing cavity, using labyrinth or floating seals and increased oil flow. The solution was effective for direct lube designs as well, but resulted in higher power loss, flow requirements, and pad temperatures comparable to a conventional, flooded design.
- The second was a modification consisting of patented SSV grooves cut in the babbitt near the edges of the pad, to capture and redirect side leakage toward the leading edge of the next pad. This solution was successful in eliminating SSV hash in an evacuated configuration. Low oil flow and power loss were maintained, with a slight penalty in pad temperature due to the introduction of warm, side leakage oil back into the oil film.
- In both cases, the elimination of SSV hash increased synchronous amplitudes.

The following conclusions are derived from the theoretical investigation of SSV hash:

- A tilting pad bearing's full coefficients can be used to assess the dynamics of individual pads.
- Using the full coefficients of one of the test bearings, theoretical investigations suggest that the observed SSV hash is likely a forced vibration phenomenon.
- Theoretical predictions indicate that a pad's responsiveness at low frequencies increases when there is insufficient oil to provide for a full film.
- At lower supply flowrates, predicted partial starvation at the leading edge progresses, which reduces the pad's tilting stiffness, making it more responsive to excitation.

DISCUSSIONS

Many questions arose over the course of the tests and analyses and during review of the initial drafts of this paper. The following discussions comment on topics that are not necessarily derived directly from the test results and analyses. As such, the discussions are subject to debate, which is welcome.

Possible Source of Excitation

Test results and analyses indicate that the shaft SSV hash indications are caused by pad vibration with response characteristics indicative of a forced vibration. Since there were no means in the SSV hash test apparatus to visualize the flow in the bearing, possible sources of excitation can only be surmised from the test results presented in this paper. Instead, attention is directed to Heshmat (1991), who did observe a periodic phenomenon in his visualization experiments of oil streamlets in an axial groove journal bearing. The phenomenon is reported as a "pulse" that periodically transformed the starved region of the leading edge film into a pattern of oil streamlets. This pulse occurred every 0.5 to 1.0 seconds and its frequency varied with the degree of starvation.

This phenomenon is consistent with many of the observations from these SSV hash investigations. Test data and analyses both show an increased sensitivity to SSV hash at reduced flowrates. A periodic pulse excitation can explain dominant SSV hash amplitudes at intermediate operating conditions, i.e., peaks noticeable in Figures 17 through 22, as well as difference in SSV hash signatures among test bearings, which may be attributable to the influence of the different supply methods on the excitation.

Pad Vibration and Damage

Pad flutter, babbitt fatigue, and pivot fretting are often brought up as topics of concern regarding SSV hash. The babbitt damage studied by Adams and Payandeh (1982) was a major concern in large, conventional, flooded bearings, attributed to self-excited, subsynchronous vibrations of unloaded pads with frequency ratios approximately 0.50 that of running speed. The term *pad flutter* is often used to describe this motion, and *spragging* is often used to describe more violent, full clearance vibrations with forces sufficient to fatigue the babbitt and fret the pivots.

The pad vibrations associated with SSV hash do not conform to these characteristics. Subsynchronous amplitudes are at least an order of magnitude less than the bearing clearance, and frequency ratios are more on the order of 0.10 on average. Babbitt fatigue is not considered a concern in regard to the SSV hash characteristics described in this paper.

Fretting is a more difficult phenomenon to assess analytically. Vibrations certainly contribute to fretting, but there are many sources of vibration in turbomachinery. The only information that can be offered from the SSV hash test series in this respect is that there were no indications of fretting, or babbitt fatigue, in individual test pads after 600 hours of operation.

Bearing Clearance, Preload, Pivot Offset

It would seem that preload, via reduced bearing clearance, would reduce shaft SSV hash and that increasing the pivot offset should make it worse. It was therefore unexpected when center versus offset pivot tests showed lower levels for offset pivot operation.

Hindsight from the test results and analyses indicate other factors are involved, e.g., proximity of the individual pads to the shaft, the magnitude of their hydrodynamic forces, sensitivity to excitation, etc., which make it difficult to generalize cause and effect. Although preload and clearance tests were not complete at the time of this paper, scenarios where preload might invoke pad vibration and shaft SSV hash can be envisioned when considering the other influences.

With multiple factors and complex pad/shaft interactions, cause and effect scenarios for clearance, preload, offset, and other geometry should be performed by analysis rather than generalizations. The analyses presented in the theory section of the paper are useful tools for assessing new designs, as well as evaluating changes to existing designs.

SSV Hash: Issue, Nonissue, Allowable Levels

The many types of turbomachinery and the wide array of sizes and operating conditions suggest caution against generalizations. There are applications running with SSV hash with no reported problems, and DeCamillo and Clayton (1997) and Edney, et al. (1996), provide rotordynamic data showing some level of flow reduction is possible without affecting rotor response. On the other hand, Edney, et al. (1996), do report problems when flow is reduced too much, which is logical and also supported by the theoretical analyses.

Personal experience with SSV hash for turbomachinery bearing sizes 3.88 to 8.00 inches (100 to 200 mm) in diameter generally falls within API guidelines. In comparisons with API 617 (2002) nonsynchronous limits, for example, levels are typically less then 0.2 mils (.0050 mm) peak-to-peak. Actually, SSV hash more often is a consideration in overall vibration limitations, as nonsynchronous frequencies are typically below 0.25 times the maximum continuous speed and are indiscrete. Noted earlier, elimination of SSV hash tended to increase synchronous amplitudes in tests. This is brought up neither as an issue or nonissue, but to provide information that overall vibration levels may not decrease as much as anticipated when SSV hash is eliminated.

Issues more often arise when other specifications further limit allowable SSV indications or, as stated earlier, because of uncertainty regarding the cause and nature of the vibration. In this case, solutions and test results in this paper can be used to address the situation. A more challenging issue is complying with multiple spec limitations in more severe applications. It seems that many of the parameters that reduce SSV hash tend to increase power loss, flow requirement, and pad temperature, or produce undesirable rotor response. Flooding and pressurized bearing cavities, rotordynamic preference for center pivot load-on-pad configurations, and tighter clearances are some examples.

There is certainly the need for more research and development, experimental and theoretical, on the subject of SSV hash including its effects on dynamic coefficients, rotor response, and stability. In the meantime, the authors hope that the tests and analytical investigations presented in this paper will provide a useful reference for topics related to SSV hash.

APPENDIX A—

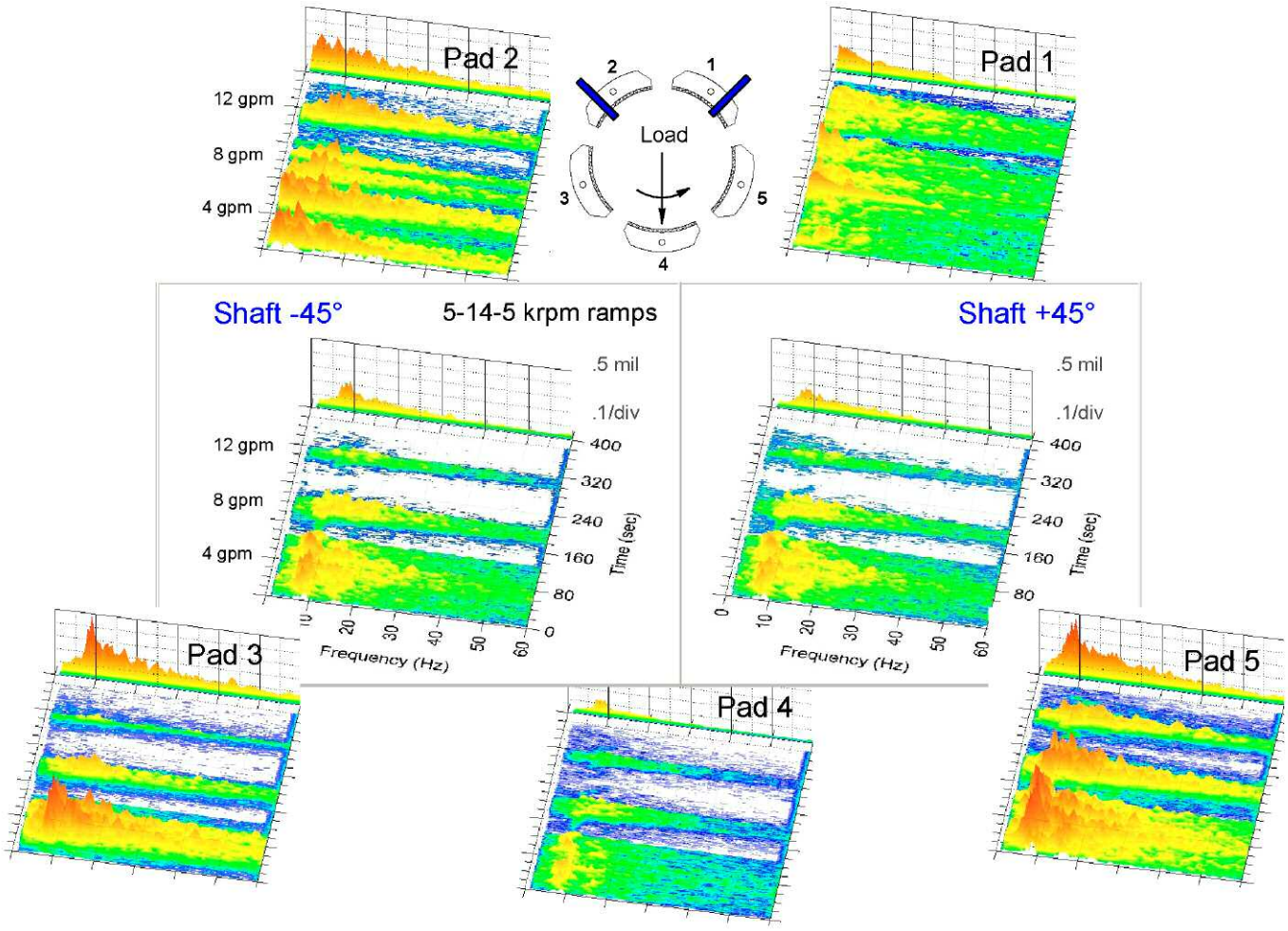

Figure A-1. Direct Lube Leading-Edge-Groove, LOP, 200 psi (1.38 MPa), No SSV Grooves.

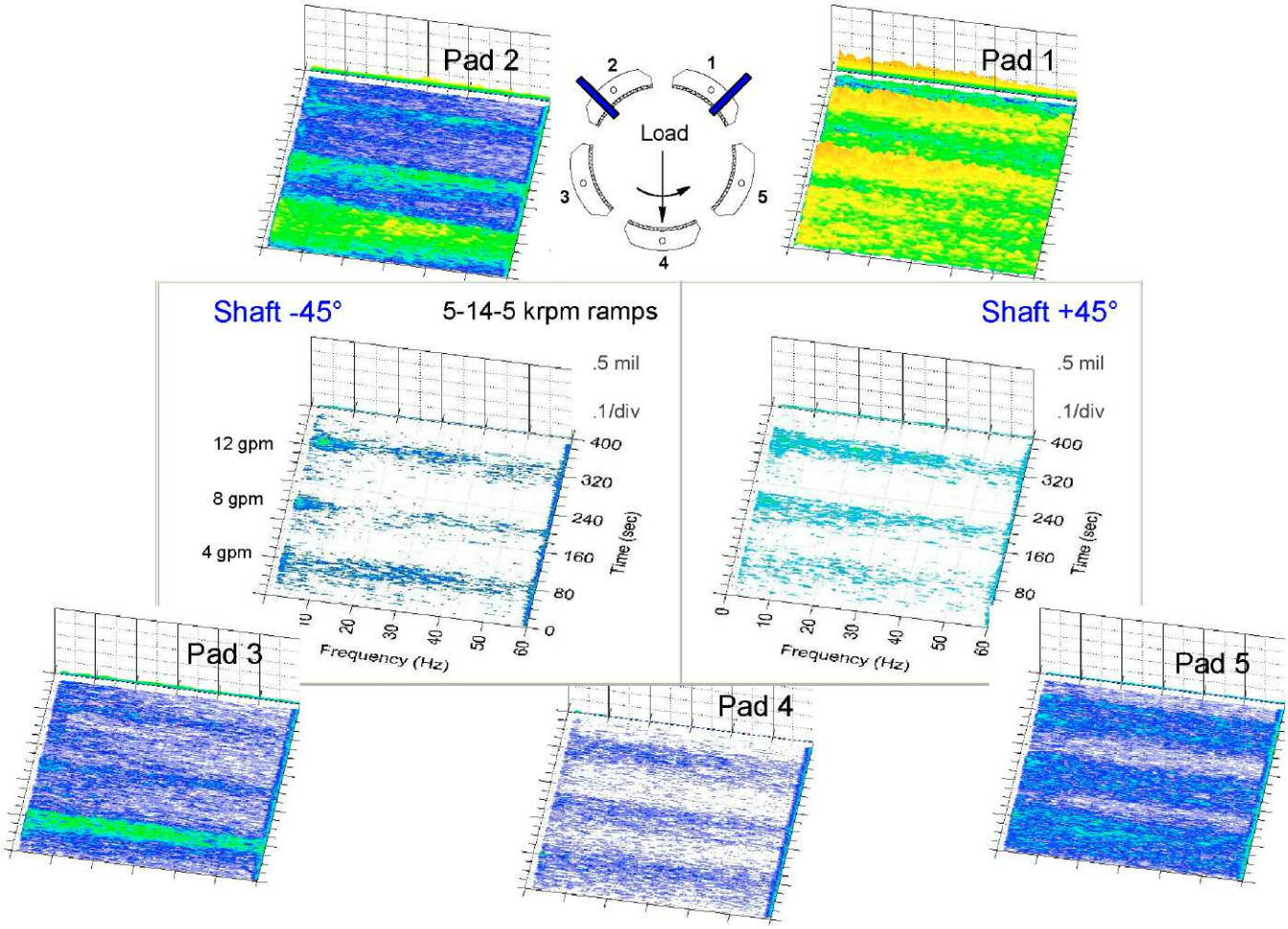

Figure A-2. Direct Lube Leading-Edge-Groove, LOP, 200 psi (1.38 MPa), with SSV Grooves.

REFERENCES

Adams, M. L. and Payandeh, S., 1983, "Self-Excited Vibration of Statically Unloaded Pads in Tilting-Pad Journal Bearings," *ASME Journal of Lubrication Technology, 105,* pp. 377-384.

API 617, 2002, "Axial and Centrifugal Compressors and Expander-Compressors for Petroleum, Chemical and Gas Industry," Seventh Edition, American Petroleum Institute, Washington, D.C.

Booser, E. R., 1990, "Parasitic Power Losses in Turbine Bearings," *STLE Tribology Transactions, 33,* pp. 157-162.

Brockwell, K., Dmochowski, W., and DeCamillo, S., 1992, "Performance Evaluation of the LEG Tilting Pad Journal Bearing," *IMechE Seminar Plain Bearings—Plain Bearings—Energy Efficiency and Design,* MEP, London, United Kingdom, pp. 51-58.

Cloud, C. H., 2007, "Stability of Rotors Supported on Tilting Pad Journal Bearings," Ph.D. Dissertation, University of Virginia, Charlottesville, Virginia.

DeCamillo, S. and Clayton, P. J., 1997, "Performance Tests of an 18-Inch Diameter, Leading Edge Groove Pivoted Shoe Journal Bearing," *Proceedings of the 2nd International Conference on Hydrodynamic Bearing—Rotor System Dynamics,* Xi'an, China, pp. 409-413.

DeCamillo, S., 2006, "Current Issues Regarding Unusual Conditions in High-Speed Turbomachinery," Keynote Presentation, *5th EDF & LMS Poitiers Workshop Bearing Behavior Under Unusual Operating Conditions Proceedings,* pp A.1-A.10.

Edney, S. L., Waite, J. K., and DeCamillo, S. M., 1996, "Profiled Leading Edge Groove Tilting Pad Journal Bearing for Light Load Operation," *Proceedings of the Twenty-Fifth Turbomachinery Symposium,* Turbomachinery Laboratory, Texas A&M University, College Station, Texas, pp. 1-16.

Fillon, M., Bligoud, J. C., and Frene, J., 1993, "Influence of the Lubricant Feeding Method on the Thermohydrodynamic Characteristics of Tilting Pad Journal Bearings," *Proceedings of the 6th International Congress on Tribology,* Budapest, Hungary, *4,* pp. 7-10.

Harangozo, A. V., Stolarski, T. A., and Gozdawa, R. J., 1991, "The Effect of Different Lubrication Methods on the Performance of a Tilting Pad Journal Bearing," *STLE Tribology Transactions, 34,* pp. 529-536.

He, M., 2003, "Thermoelastohydrodynamic Analysis of Fluid Film Journal Bearings," Ph.D. Dissertation, University of Virginia, Charlottesville, Virginia.

He, M., Cloud, C. H., and Byrne, J. M., 2005, "Fundamentals of Fluid Film Journal Bearing Operation and Modeling," *Proceedings of the Thirty-Fourth Turbomachinery Symposium,* Turbomachinery Laboratory, Texas A&M University, College Station, Texas, pp. 155-175.

Heshmat, H., 1991, "The Mechanism of Cavitation in Hydrodynamic Lubrication," *STLE Tribology Transactions, 34,* (2), pp. 177-186.

Kocur, J. A., Nicholas, J. C., and Lee, C. C., 2007, "Surveying Tilting Pad Journal Bearing and Gas Labyrinth Seal Coefficients and Their Effect on Rotor Stability," *Proceedings of the Thirty-Sixth Turbomachinery Symposium,* Turbomachinery Laboratory, Texas A&M University, College Station, Texas, pp. 1-10.

Parsell, J. K., Allaire, P. E., and Barrett, L. E., 1983, "Frequency Effects in Tilting-Pad Journal Bearing Dynamic Coefficients," *ASLE Transactions, 26,* (2), pp. 222-227.

Shapiro, W. and Colsher, R., 1977, "Dynamic Characteristics of Fluid-Film Bearings," *Proceedings of the Sixth Turbomachinery Symposium,* Turbomachinery Laboratory, Texas A&M University, College Station, Texas, pp. 39-53.

Tanaka, M., 1991, "Thermohydrodynamic Performance of a Tilting Pad Journal Bearing with Spot Lubrication," *ASME Journal of Tribology, 113,* pp. 615-619.

Wilkes, J. J., DeCamillo, S. M., Kuzdzal, M. J., and Mordell, J. D., 2000, "Evaluation of a High Speed, Light Load Phenomenon in Tilting-Pad Thrust Bearings," *Proceedings of the Twenty-Ninth Turbomachinery Symposium,* Turbomachinery Laboratory, Texas A&M University, College Station, Texas, pp. 177-185.

Wilkes, J. and DeCamillo, S., 2002, "Journal Bearing," United States Patent No. 6,361,215 B1, Mar. 26, 2002.

ACKNOWLEDGEMENT

The authors would like to thank colleagues at Kingsbury, Inc., for their special efforts and help in acquiring and preparing data and information for this technical paper. The authors would also like to especially acknowledge John Kocur of ExxonMobil, Brian Pettinato of Elliott, and Thomas Soulas of Dresser-Rand, among others, for their help and expertise in discussions of the subject matter.

JOURNAL BEARING VIBRATION AND SSV HASH

by

Scan M. DeCamillo

Manager, Research and Development

Kingsbury, Inc.

Philadelphia, Pennsylvania

Minhui He

Machinery Specialist

C. Hunter Cloud

President

and

James M. Byrne

Machinery Consultant

BRG Machinery Consulting, LLC

Charlottesville, Virginia 22903 USA

Scan M. DeCamillo is Manager of Research and Development for Kingsbury, Inc., in Philadelphia, Pennsylvania. He is responsible for design, analysis, and development of Kingsbury fluid film bearings for worldwide industrial and military applications. He began work in this field in 1975 and has since provided engineering support to industry regarding application and performance of hydrodynamic bearings. Mr. DeCamillo has developed performance and structural bearing analysis tools during his career, establishing design criteria used in many publications and specifications. He has patents and has authored several papers on bearing research, which is currently focused on advancing hydrodynamic bearing technology in high-speed turbomachinery.

Mr. DeCamillo received his B.S. degree (Mechanical Engineering, 1975) from Drexel University. He is a registered Professional Engineer in the State of Pennsylvania and a member of STLE, ASME, and the Vibration Institute.

Minhui He is a Machinery Specialist with BRG Machinery Consulting LLC, in Charlottesville, Virginia. His responsibilities include vibration troubleshooting, rotor-dynamic analysis, as well as bearing and seal analysis and design. He is a member of STLE, and is also conducting research on rotordynamics and hydrodynamic bearings.

Dr. He received his B.S. degree (Chemical Machinery Engineering, 1994) from Sichuan University. From 1996 to 2003, he conducted research on fluid film journal bearings in the ROMAC Laboratories at the University of Virginia, receiving his Ph. D. (Mechanical and Aerospace Engineering, 2003).

C. Hunter Cloud is President of BRG Machinery Consulting, LLC, in Charlottesville, Virginia, a company providing a full range of rotating machinery technical services. He began his career with Mobil Research and Development Corporation in Princeton, NJ, as a turbomachinery specialist responsible for application engineering, commissioning, and troubleshooting for production, refining, and chemical facilities. During his 11 years at Mobil, he worked on numerous projects, including several offshore gas injection platforms in Nigeria, as well as serving as reliability manager at a large US refinery.

Dr. Cloud received his B.S. (Mechanical Engineering, 1991) and Ph.D. (Mechanical and Aerospace Engineering, 2007) from the University of Virginia. He is a member of ASME, the Vibration Institute, and the API 684 rotordynamics task force.

James M. Byrne is currently a member of the BRG Machinery Consulting team, in Charlottesville, Virginia. BRG performs research and analysis in the fields of fluid film bearings, magnetic bearings, and rotordynamics. Mr. Byrne began his career designing internally geared centrifugal compressors for Carrier in Syracuse, New York. He continued his career at Pratt and Whitney aircraft engines and became a technical leader for rotordynamics. Later Mr. Byrne became a program manager for Pratt and Whitney Power Systems managing the development of new gas turbine products. From 2001 to 2007, he was President of Rotating Machinery Technology, a manufacturer of tilting pad bearings.

Mr. Byrne holds a BSME degree from Syracuse University, an MSME degree from the University of Virginia, and an MBA from Carnegie Mellon University.